JACS
JOURNAL OF THE AMERICAN CHEMICAL SOCIETY
Article
pubs.acs.org/JACS

Putting the Squeeze on CH_4 and CO_2 through Control over Interpenetration in Diamondoid Nets

Sameh K. Elsaidi,[†,⊥,‡] Mona H. Mohamed,[†,⊥,‡] Lukasz Wojtas,[†] Anjana Chanthapally,[§] Tony Pham,[†] Brian Space,[†] Jagadese J. Vittal,[§] and Michael J. Zaworotko*[,†]

[†]Department of Chemistry, CHE205, University of South Florida, 4202 East Fowler Avenue, Tampa, Florida 33620, United States
[⊥]Chemistry Department, Faculty of Science, Alexandria University, P.O. Box 426 Ibrahimia, Alexandria 21321, Egypt
[§]Department of Chemistry, National University of Singapore, Singapore 117543

Supporting Information

ABSTRACT: We report the synthesis, structure, and sorption properties of a family of eight diamondoid (**dia**) metal–organic materials (MOMs) that are sustained by Co(II) or Zn(II) cations linked by one of three rigid ligands: 4-(2-(4-pyridyl)ethenyl)benzoate (**1**), 4-(pyridin-4-yl)benzoate (**2**), and 4-(pyridin-4-yl)acrylate (**3**). Pore size control in this family of **dia** nets was exerted by two approaches: changing the length of the linker ligand from **1** to **3**, and using solvent as a template to control the level of interpenetration in nets based upon **1** and **3**. The resulting MOMs, dia-8i-**1**, dia-5i-**3**, dia-7i-**1**-Zn, dia-7i-**1**-Co, dia-4i-**3**-a, dia-4i-**3**-b, dia-4i-**2**, and dia-4i-**1**, exhibit 1D channels with pore limiting diameters (PLDs) of 1.64, 2.90, 5.06, 5.28, 8.57, 8.83, 11.86, and 18.25 Å, respectively. We selected **dia** nets for this study for the following reasons: their 1D channels facilitate study of the impact of pore size on gas sorption parameters in situations where pore chemistry is similar (pyridyl benzoate-type linkers) or identical (in the case of polymorphs), and their saturated metal centers eliminate open metal sites from dominating sorbent–solvate interactions and possibly masking the effect of pore size. Our data reveal that smaller pore sizes offer stronger interactions, as determined by the isosteric heat of adsorption (Q_{st}) and the steepness of the adsorption isotherm in the low-pressure region. The porous MOM with the smallest PLD suitable for physisorption, dia-7i-**1**-Co, was thereby found to exhibit the highest Q_{st} values for CO_2 and CH_4. Indeed, dia-7i-**1**-Co exhibits a Q_{st} for CH_4 of 26.7 kJ/mol, which was validated through grand canonical Monte Carlo simulation studies of CH_4 adsorption. This Q_{st} value is considerably higher than those found in covalent organic frameworks and other MOMs with unsaturated metal centers. These results therefore further validate the critical role that PLD plays in gas adsorption by porous MOMs.

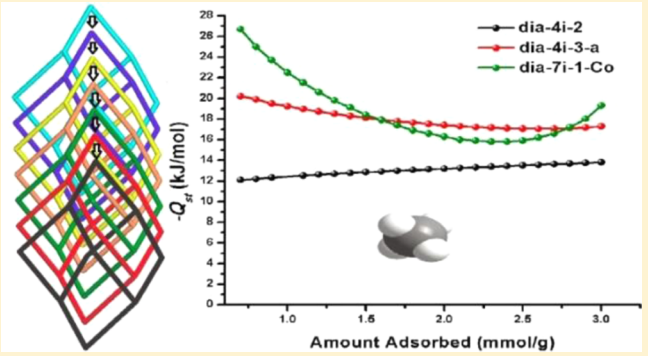

INTRODUCTION

Natural gas (NG), which is predominantly methane, is the most abundant source of hydrocarbon fuel and offers several advantages over liquid and solid hydrocarbon fuels: 30–40% lower carbon footprint, 60–80% less smog-producing pollutants, and lower cost. However, the current technologies for storage and transportation of NG, compressed NG and liquefied NG, face considerable hurdles to their more widespread adoption because of the challenges and costs associated with pressurization and cooling, respectively. In addition, NG is typically contaminated with CO_2 and H_2S, which should be reduced in concentration to "sweeten" NG prior to use. The development of technologies for NG storage/purification and carbon capture based upon porous materials has been intensely studied in recent years with emphasis upon zeolites,[1] porous activated carbon and carbon nanotubes,[2−4] covalent organic frameworks (COFs),[5] and metal–organic materials (MOMs).[6−8] Their structures (especially their modularity) and properties (especially permanent porosity)[9−11] also make MOMs a particularly attractive class of materials for applications beyond gas storage and separation,[12] including heterogeneous catalysis,[13] drug delivery,[14] and conductivity.[15] In the context of gas storage, MOMs for hydrogen storage have not yet come close to U.S. Department of Energy (DOE) targets.[16] In contrast, NG storage is more promising,[17,18] since there are already MOMs that meet an early DOE target for volumetric uptake of CH_4 (180 cm^3/cm^3 at 298 K, 35 bar).[17] The newer DOE target for volumetric CH_4 uptake is 263 cm^3/cm^3 (298 K, 65 bar), and it was recently reported that the prototypal MOMs HKUST-1 and Ni-MOF-74 exhibit CH_4 uptake of 270 and 250 cm^3/cm^3, respectively, at these conditions.[19,20] Ni-MOF-74 outperforms HKUST-1 at lower pressure (<35 bar) because of its high isosteric heat of

Received: January 1, 2014
Published: March 10, 2014

   dx.doi.org/10.1021/ja500005k | J. Am. Chem. Soc. 2014, 136, 5072–5077

adsorption (Q_{st}) of 21.4 kJ/mol (HKUST-1 exhibits Q_{st} = 17 kJ/mol). Recent studies concerning selective carbon capture in a family of MOMs sustained by saturated metal centers (SMCs)[21,22] revealed the profound effect that pore size can impart upon CO_2 capture performance.

In order to further optimize performance for NG purification and storage, it is necessary to address both the energetics of gas sorption and surface area. Herein we address the matter of energetics by reporting how systematic pore size control through crystal engineering can be accomplished in diamondoid (**dia**) MOMs with SMCs. A new benchmark for the isosteric heat of sorption for CH_4, Q_{st} = 26.7 kJ/mol, was thereby observed along with confirmation of the modulating effect of pore size. Our experimental results and accompanying theoretical studies[22] further indicate that optimal pore size lies in the range 4−8 Å, or just above the kinetic diameter of CH_4 (3.8 Å).[17,23,24] MOMs with smaller pore size typically exhibit relatively high uptake of CH_4 in the lower pressure region (1−40 bar) because of stronger interactions between CH_4 molecules and the framework (as measured by higher Q_{st} values). In contrast, MOMs with large pore limiting diameters (PLDs) are better suited for higher pressure uptake (40−200 bar).[17] The Q_{st} across the range of loadings also plays a critical role in CH_4 storage applications. When CH_4 is utilized for vehicle operation, it is desirable to have a high Q_{st} value at the charging pressure and a low Q_{st} value at the discharging pressure.[25] In contrast, a relatively high Q_{st} value at low pressure is optimal for other applications, such as storage of CH_4 in tanks, CH_4 purification, and CH_4 biofiltration. Therefore, in order to generate MOMs that are optimal for such applications, it is necessary to fully understand how to optimize both pore size and chemistry. In this contribution, we focus upon the matter of pore size through the systematic study of a family of **dia** networks formed by complexation of the ligands L1−L3 to Co(II) or Zn(II) (see Figure 1).

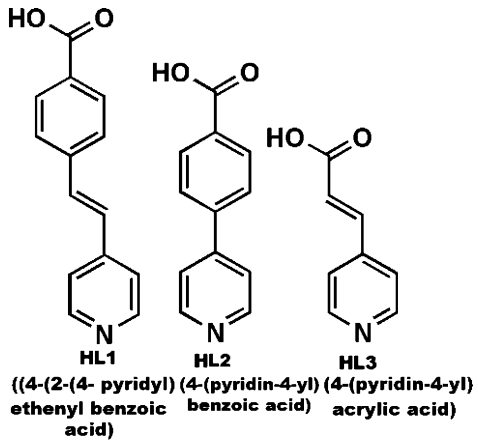

Figure 1. Ligands (**HL1**−**HL3**) used herein for the synthesis of **dia** nets.

EXPERIMENTAL SECTION

All reagents were used as purchased. Solvents were purified according to standard methods and stored in the presence of molecular sieves. Powder X-ray diffraction (PXRD) data were recorded at 298 K on a Bruker D8 Advance X-ray diffractometer at 20 kV, 5 mA for Cu KR (λ = 1.5418 Å), with a scan speed of 0.5 s/step (6°/min) and a step size of 0.05° in 2θ. Calculated PXRD patterns were produced using Powder Cell for Windows Version 2.4 (programmed by W. Kraus and G. Nolze, BAM Berlin, 2000). Gas adsorption isotherms were measured on a Micromeritics ASAP 2020 surface area and porosity analyzer.

Co(L1)$_2$, dia-4i-**1**, was afforded by solvothermal reaction at 105 °C of 0.10 mmol (0.029 g) of $Co(NO_3)_2{\cdot}6H_2O$ and 0.20 mmol (0.048 g) of **HL1** in 15 mL of *tert*-butylformamide/*tert*-butyl alcohol (2:1 ratio). Red, needle-like crystals of dia-4i-**1** were harvested after 24 h (yield 40%, 0.10 g based on $Co(NO_3)_2$). Single-crystal X-ray crystallography revealed that dia-4i-**1** crystallizes in the orthorhombic space group *F*222 (a = 12.8020(3) Å, b = 34.9232(8) Å, c = 43.7551(1) Å, V = 19562.3 Å^3). TOPOS revealed four independent networks related by two translation vectors, [0.5,0.5,0] and [0.5,−0.5,0]. Adjacent nets are separated through these vectors at 18.60 Å. Dia-4i-**1** exhibits rectangular channels parallel to [1,0,0] with a PLD of 18.25 Å. The PLD values reported herein represent the accessible pore size as obtained by measuring the longest diagonal of the channel and subtracting 3.5 Å for van der Waals distances.

Co(L1)$_2$, dia-7i-**1**-Co, was synthesized via the same method as that used for dia-4i-**1** except DMF/EtOH was used as solvent. Red, rod-shaped crystals of dia-7i-**1**-Co were harvested after 24 h (yield 62%, 0.13 g based on $Co(NO_3)_2$). Dia-7i-**1**-Co crystallizes in the monoclinic space group *Cc* with a = 13.337(1) Å, b = 24.979(2) Å, c = 8.5046(7) Å, V = 2797.56 Å^3. Seven independent networks are interpenetrated, with a translational vector corresponding to the crystallographic c axis (8.50 Å) (Figure 2a). Dia-7i-**1**-Co exhibits narrow pores along [001] with PLDs of 5.28 Å.

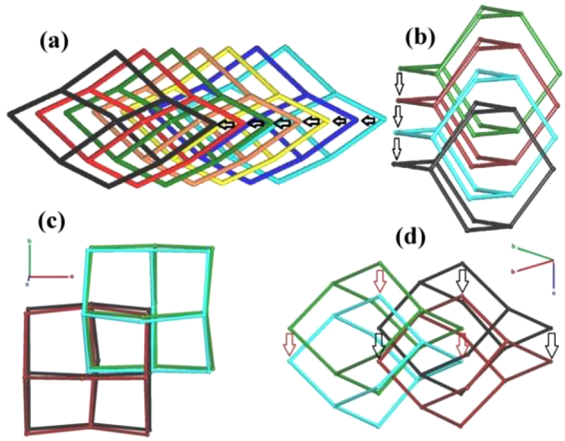

Figure 2. (a,b) Illustrations of interpenetration in class Ia nets that are related by a single translation via a full interpenetration vector: (a) 7-fold interpenetrated nets and (b) 4-fold-interpenetrated nets. (c,d) Illustrations of class IIIa **dia** nets which are related by translation and nontranslation symmetry operations; the four interpenetrated nets can be described as two sets of 2-fold nets (2+2).

Zn(L1)$_2$, dia-7i-**1**-Zn, is isostructural with dia-7i-**1**-Co and was synthesized via similar procedures (see Supporting Information).

Co(L1)$_2$, dia-8i-**1**, was synthesized via the same reaction method as used for dia-4i-**1**, except DMA/EtOH was used as solvent. Dark red triangular crystals were isolated after 24 h (yield 54%, 0.12 g based on $Co(NO_3)_2$). Dia-8i-**1** crystallizes in the orthorhombic space group *Aba*2 (a = 13.1543(8) Å, b = 21.7445(11) Å, c = 8.6774(6) Å, V = 2482.03 Å^3) and exhibits 8-fold interpenetration with nets related by a translation vector of 11.55 Å along [0,0.5,0.5] and [0,0.5,−0.5]. Dia-8i-**1** exhibits pores along [1,0,0] with PLD of only 1.643 Å. Isostructural variants of dia-7i-**1**-Co and dia-8i-**1** have been reported previously.[26,27]

Co(L2)$_2$, dia-4i-**2**, was prepared by reaction of 0.10 mmol (0.029 g) of $Co(NO_3)_2$ and 0.20 mmol (0.040g) of **HL2** in 15 mL of DMF at 105 °C for 24 h, yielding red, needle-like crystals (yield 65%, 0.13 g based on $Co(NO_3)_2$). Dia-4i-**2** crystallizes in the tetragonal space group $P4_12$ with a = b = 22.6250(7) Å, c = 12.7634(5) Å, V = 6533.46 Å^3.

dx.doi.org/10.1021/ja500005k | J. Am. Chem. Soc. 2014, 136, 5072−5077

Scheme 1. Schematic Representation of the Control over the Level of Interpenetration in dia Nets Achieved via Solvent Templation

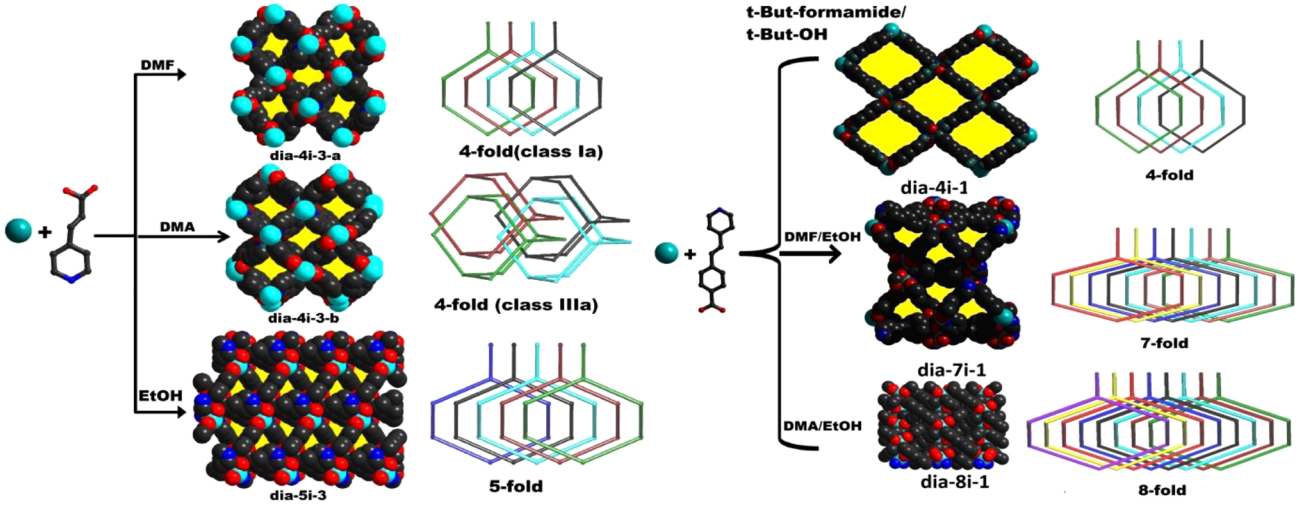

Analysis using TOPOS revealed that dia-4i-**2** is a class IIIa **dia** net with two sets of 2-fold nets (Figure 2c,d). The interpenetration vector in each set is parallel to the *c* axis with a relative displacement 11.88 Å, and it can be described as a (2+2) interpenetrated **dia** system.[28] Dia-4i-**2** exhibits rectangular channels along the *c* axis with a PLD of 11.86 Å.

Co(L3)$_2$, dia-4i-**3**-a, was prepared by reaction of 0.10 mmol (0.029 g) of $Co(NO_3)_2$ and 0.20 mmol (0.040 g) of **HL3** in 15 mL of DMF at 105 °C for 24 h. Dark red, rod-like crystals were isolated (yield 60%, 0.12 g based on $Co(NO_3)_2$). Dia-4i-**3**-a crystallizes in the tetragonal space group $P42_12$, with $a = b$ =17.4848(8) Å, c = 20.2126(9) Å, and V = 6179.32 Å^3. It exhibits four interpenetrated nets that are related by two translation vectors parallel to the *c* axis and separated by 20.33 Å. Rectangular channels lie parallel to the [0,0,1] direction with a PLD of 8.57 Å.

Co(L3)$_2$, dia-4i-**3**-b, was synthesized via the same reaction method as that used for dia-4i-**3**-a, except DMA was used as solvent. Rectangular purple crystals were isolated after 24 h (yield 54%, 0.11 g based on $Co(NO_3)_2$). Dia-4i-**3**-b crystallizes in the orthorhombic space group *Pnna* with a = 12.4892(15) Å, b = 13.6324(15) Å, c = 12.1687(15) Å, and V = 2071.82 Å^3. TOPOS revealed that the interpenetration is class IIIa, the same as that exhibited by dia-4i-**2**. The interpenetration vector is parallel to the *c* axis with a relative displacement 12.07 Å, and the structure can be described as (2+2) interpenetration. The interpenetrated nets are equally separated along [010] by 6.944(12) Å. Dia-4i-**3**-b exhibits rectangular channels along [010] with a PLD of 8.83 Å.

Co(L3)$_2$, dia-5i-**3**, was synthesized via the same reaction method as that used for dia-4i-**3**-a except EtOH was the solvent. Red triangular crystals were isolated after 24 h (yield 48%, 0.10 g based on $Co(NO_3)_2$). Dia-5i-**3** crystallizes in the monoclinic space group *Cc* with a = 11.6908(4) Å, b = 21.0100(6) Å, c = 8.5286(2) Å, and V = 1588.33 Å^3). The structure of dia-5i-**3** consists of 5-fold interpenetrated **dia** nets, with a translation parallel to the crystallographic *c* axis of 8.34 Å. Dia-5i-**3** exhibits narrow pores parallel to [001] with PLDs of 2.7 Å (see SI for full crystallographic details).

RESULTS AND DISCUSSION

We selected **dia** nets for our study because of their amenability to design, relative ease of synthesis, and absence of unsaturated metal centers (UMCs). UMCs can enhance gas selectivity and storage capacity, as exemplified by Mg/DOBDC[29] (DOBDC = 2,5-dihydroxyterephthalate), the Mg analogue of MOF-74,[30] and CPO-27-Zn,[31] which exhibits high CO_2 storage capacity (35.2 wt% at 298 K, 1 atm), high Q_{st} (47 at zero loading), and high selectivity for CO_2 over CH_4 (11.5 at 1 atm). However, there are high energy costs for activating and regenerating MOMs with UMCs, at least in part because they tend to exhibit high affinity toward H_2O. Further, UMCs can mask the effect of pore size. MOMs with SMCs rely upon weaker molecular recognition forces (physisorption) and therefore represent an attractive platform for directly testing the impact of pore size upon Q_{st}.

Several MOM families or "platforms" with SMCs have already been extensively studied in the context of CO_2 and CH_4 sorption, in particular, zeolitic imidazolate frameworks (ZIFs)[32,33] and pillared square grid MOMs.[21] **Dia** nets represent a platform which has not yet been well studied in terms of gas adsorption, despite being one of the earliest and most widely studied classes of MOMs from a structural perspective.[34] This is presumably because **dia** nets tend to exhibit interpenetration,[35−37] which mitigates against high surface area and increases density. However, there are studies which indicate that interpenetration in MOMs that are topologically amenable to interpenetration can be controlled.[38−41] Further, nets of general formula $[Co(L)_2]$, L = a pyridylcarboxylate ligand, can afford a rich diversity of pore sizes and levels of interpenetration, as exemplified by the variants prepared for this study: dia-8i-**1** (8-fold interpenetration, L1); dia-5i-**3** (5-fold interpenetration, L3); dia-7i-**1**-Co (7-fold interpenetration, L1); dia-7i-**1**-Zn (7-fold interpenetration, L1); dia-4i-**3**-a (4-fold interpenetration, L3); dia-4i-**3**-b (4-fold interpenetration, L3); dia-4i-**2** (4-fold interpenetration, L2); and dia-4i-**1** (4-fold interpenetration, L1). 1D channels exhibiting PLDs of 1.64, 2.90, 5.28, 8.57, 8.83, 11.86 and 18.25 Å, respectively, were afforded in this family of **dia** nets. Notably, dia-8i-**1**, dia-7i-**1**-Co, and dia-4i-**1** are polymorphs, as are dia-4i-**3**-a, dia-4i-**3**-b, and dia-5i-**3**. A comparison between polymorphs facilitates an "apples-to-apples" comparison of the effect of pore size upon gas sorption.

Pore size control in **dia** nets is addressed herein through the use of two crystal engineering strategies.[42] The first approach uses solvent as a template to control the level of interpenetration during the reaction of **HL1** or **HL3** with $Co(NO_3)_2$ at 105 °C, thereby affording two sets of three polymorphs: dia-4i-**1** (4-fold), dia-7i-**1**-Co (7-fold), and dia-8i-**1** (8-fold) from **HL1** and dia-4i-**3**-a (4-fold), dia-4i-**3**-b (4-fold), and dia-5i-**3**

dx.doi.org/10.1021/ja500005k | J. Am. Chem. Soc. 2014, 136, 5072−5077

(5-fold) from **HL3** (Scheme 1). Dia-4i-**1**, dia-7i-**1**-Co, and dia-8i-**1** were evaluated through TOPOS,[43,44] which revealed that the nets belong to class 1a (Figure 2a,b).[28] *tert*-Butylformamide afforded dia-4i-**1**, the polymorph with the largest void volume and PLD (18.25 Å). The use of less bulky solvents, DMF and DMA, afforded dia-7i-**1**-Co and dia-8i-**1**, analogues with much narrower channels (PLDs of 5.28 and 1.64 Å, respectively). Dia-4i-**3**-a, dia-4i-**3**-b, and dia-5i-**3** were also analyzed by TOPOS, which revealed that dia-4i-**3**-a and dia-4i-**3**-b are 4-fold interpenetrated but in different modes. Dia-4i-**3**-a exhibits class Ia interpenetration in which the nets are related by translational symmetry operations (Figure 2b), whereas dia-4i-**3**-b belongs to class IIIa;[28] i.e., the nets are related by both translational and nontranslational symmetry operations (Figure 2c,d). Dia-5i-**3** exhibits 5-fold interpenetration and belongs to class 1a. The exploitation of DMF and DMA as solvent and template afforded dia-4i-**3**-a and dia-4i-**3**-b with PLD values of 8.54 and 8.78 Å, respectively, while EtOH, a less bulky solvent, afforded dia-5i-**3** and much smaller pores (2.90 Å). To our knowledge, this is the first study that demonstrates how crystallization solvent can systematically and rationally impact the level of interpenetration exhibited by **dia** nets. Such an approach could well be generally applicable toward control over interpenetration. Perhaps more importantly, such control facilitates study of the impact of pore size upon gas sorption in polymorphs. The second approach used herein for control of pore size was a more traditional crystal engineering approach;[45,46] the use of linker ligands of varying length. **HL1**, **HL2**, and **HL3** afforded four **dia** nets with the same levels of interpenetration (4-fold) and similar pore chemistry, dia-4i-**1**, dia-4i-**2**, dia-4i-**3**-b, and dia-4i-**3**-a, but drastically different PLDs of 18.25, 11.86, 8.83, and 8.57 Å, respectively.

The variable PLDs of the eight **dia** nets detailed herein facilitated systematic evaluation of the effect of pore size on CH_4 adsorption. The volumetric CH_4 uptakes (298 K, 35 bar) in dia-7i-**1**-Co, dia-4i-**3**-a, and dia-4i-**2** were observed to be 95, 93, and 153 cm^3/cm^3, respectively (corresponding to PLDs of 5.28, 8.57, and 11.86 Å, respectively). The Q_{st} values for CH_4 were calculated from adsorption data collected at 298, 273, and 248 K for dia-4i-**3**-a and dia-4i-**2** using three methods: the Clausius−Clapeyron equation, the Langmuir−Freundlich equation, and the virial equation. Selected gas adsorption isotherms are presented in Figure 3. Gas sorption isotherms for dia-7i-**1**-Co, the **dia** net that was found to exhibit the strongest interactions toward CH_4, were collected three times using three different samples to ensure reproducibility. Further, the isotherms were measured over a wide range of temperatures, 298, 273, 248, and 223 K. Q_{st} was calculated using the experimental sorption isotherms (see SI).

The material with the smallest PLD in this group was found to exhibit much stronger interactions with CH_4 than those with larger pore size: Q_{st} values of 26.7, 20.2, and 12.1 kJ/mol at low loading for dia-7i-**1**-Co, dia-4i-**3**-a, and dia-4i-**2**, respectively (Figure 4). Interestingly, the measured Q_{st} value for methane (26.7 kJ/mol) in dia-7i-**1**-Co, the compound with the narrowest accessible pores (5.28 Å), is the highest value yet reported for CH_4 adsorption. Indeed, the Q_{st} value at low loading surpasses even those of MOMs with UMCs, such as HKUST-1,[19] Mg-MOF-74,[17,47] Co-MOF-74,[17,47] Ni-MOF-74,[19] Mn-MOF-74[17,47] Zn-MOF-74,[17,47] PCN-14,[19] and UTSA-20,[19] which exhibit Q_{st} values of 17, 18.5, 19.6, 21.4, 19.1, 18.3, 18.7, and 18.2 kJ/mol, respectively. This value is also higher than those of covalent organic frameworks[18,48] such as

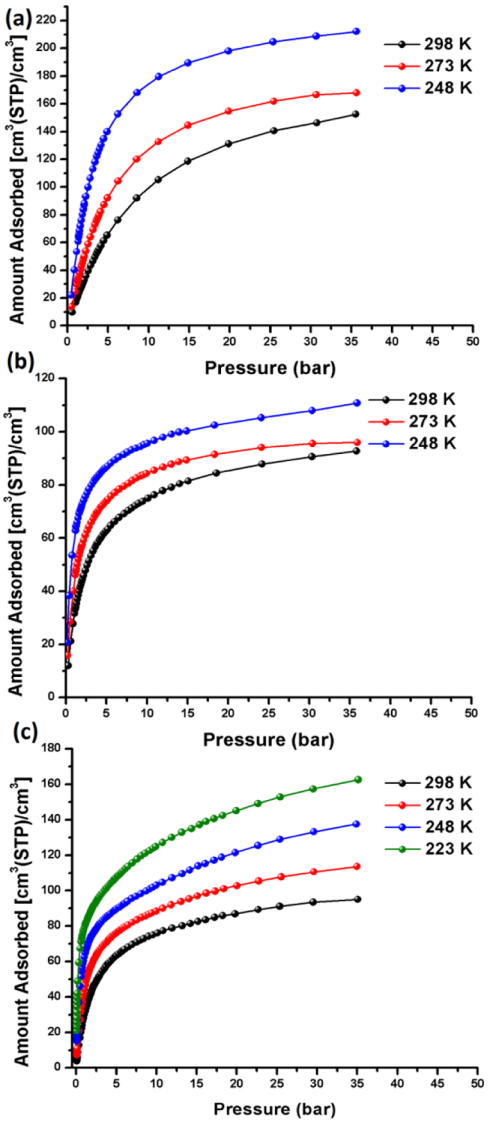

Figure 3. (a,b) Volumetric CH_4 uptake isotherms measured at 298, 273, and 248 K for (a) dia-4i-**2** and (b) dia-4i-**3**-a. (c) Volumetric CH_4 uptake isotherms measured at 298, 273, 248, and 223K for dia-7i-**1**-Co.

COF-1, COF-5, COF-6, COF-8, COF-10, COF-102, and COF-103, which exhibit Q_{st} values of 17, 8.5, 19, 12, 8.5, 8.6, and 9.5 kJ/mol, respectively. Similar uptakes at high pressures were observed for porous aromatic frameworks (PAFs), which also exhibit **dia** topology and various levels of interpenetration.[49] This result was validated through grand canonical Monte Carlo (GCMC) simulation studies of CH_4 adsorption in dia-7i-**1**-Co (see Supporting Information).

These observations prompted us to evaluate other gases such as CO_2 and H_2 with the same series of nets and the Zn analogue of dia-7i-**1**-Co, dia-7i-**1**-Zn. Dia-4i-**1**and dia-4i-**2** were found to exhibit CO_2 uptakes of 173 and 168.5 cm^3/g and 96 and 105.4 cm^3/g near 1 atm at 273 and 298 K, respectively. The CO_2 adsorption isotherms measured at 273 and 298 K in dia-4i-**3**-a and dia-7i-**1**-Co are suggestive of strong affinity toward CO_2 because of the relatively steep CO_2 uptake in the low-pressure regions compared to those seen for dia-4i-**1** and dia-4i-**2**. This is also consistent with the smaller PLDs of dia-4i-**3**-a and dia-7i-**1**-Co, promoting strong sorbent−sorbate interactions. The CO_2 uptakes of dia-4i-**3**-a at 1 atm were found to be

dx.doi.org/10.1021/ja500005k | J. Am. Chem. Soc. 2014, 136, 5072−5077

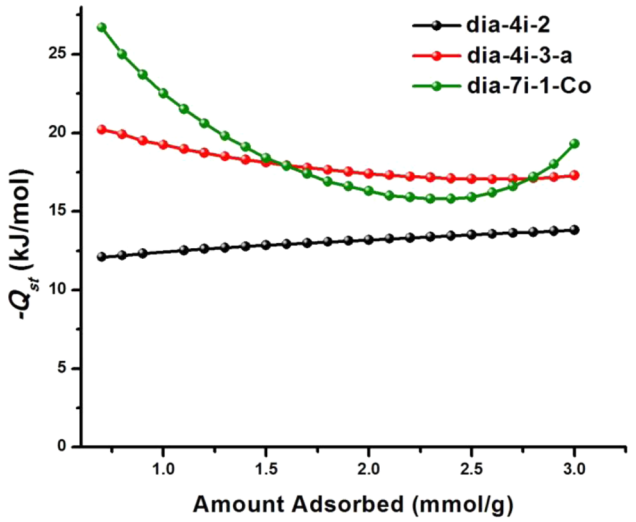

Figure 4. Isosteric heats of adsorption as a function of methane uptake for dia-7i-**1**-Co, dia-4i-**3**-a, and dia-4i-**2**.

69.8 and 90.5 cm^3/g at 298 and 273 K, respectively, whereas those of dia-7i-**1**-Co were found to be 54.8 and 74.8 cm^3/g at 298 and 273 K, respectively. Since dia-4i-**3**-a and dia-4i-**3**-b are isostructural with similar PLDs, we selected dia-4i-**3**-a for more detailed study (gas adsorption isotherms for dia-4i-**3**-b are presented in SI). The Q_{st} values for CO_2 were determined using adsorption data collected at 273 and 298 K (see SI for full details) and revealed values for dia-7i-**1**-Co, dia-4i-**3**-a, dia-4i-**2**, and dia-4i-**1** of 30, 25, 22, and 19 kJ/mol at zero loading, respectively. The CO_2 Q_{st} data further demonstrate the effect that pore size can impart upon the strength of sorbent–sorbate interactions (Figure 5).

Dia-7i-**1**-Co, dia-7i-**1**-Zn, and dia-4i-**3**-a were found to exhibit sharp increases in H_2 uptake in the low-pressure region when compared to those seen for dia-4i-**1** and dia-4i-**2** (see SI for more details). Overall, the sorption results for CH_4, CO_2, and H_2 reveal that small pore size enhances sorbent–sorbate interactions in the low-pressure region. Notably, the pore

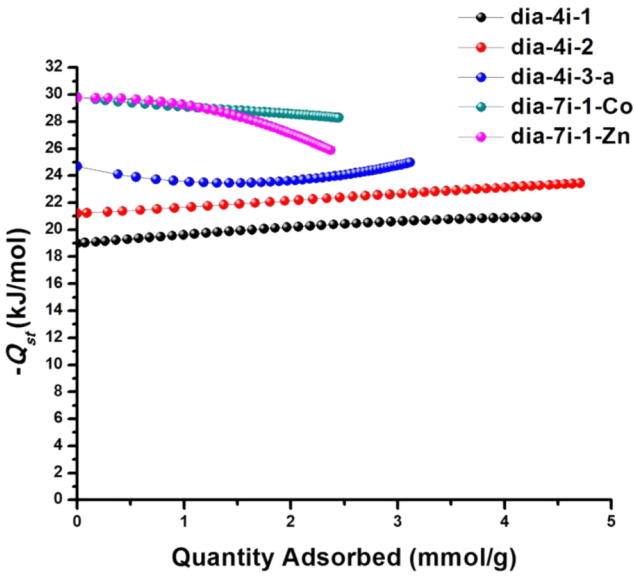

Figure 5. CO_2 isosteric heats of adsorption (Q_{st}) for dia-4i-**1**, dia-4i-**2**, dia-4i-**3**-a, dia-7i-**1**-Co, and dia-7i-**1**-Zn.

chemistry of all structures described herein is similar or identical (for polymorphs), and the presence of SMCs eliminates the possibility that open metal sites can dominate sorbent–solvate interactions and thereby mask the effect of pore size.

CONCLUSION

In summary, we have demonstrated two relatively facile strategies to modulate the pore size of **dia** networks: exploitation of solvent as a template to control the level of interpenetration, and the use of linkers with different lengths to afford nets with the same degree of interpenetration but different PLDs. This has enabled a systematic study of the impact of PLD upon gas adsorption in **dia** nets with SMCs. The porous MOMs with the smallest PLD were found to exhibit the highest Q_{st} for CH_4 and CO_2 and the highest selectivity for CO_2 over N_2. Whereas narrow PLD/high Q_{st} materials might not exhibit the highest volumetric uptakes at higher pressures and be of utility with respect to on-board vehicle storage of natural gas, they direct us toward defining PLDs that offer optimal physicochemical properties for natural gas purification and storage.

ASSOCIATED CONTENT

Supporting Information

Additional gas adsorption isotherms and crystallographic tables. This material is available free of charge via the Internet at http://pubs.acs.org.

AUTHOR INFORMATION

Corresponding Author

xtal@usf.edu

Author Contributions

‡S.K.E. and M.H.M. contributed equally.

Notes

The authors declare no competing financial interest.

ACKNOWLEDGMENTS

M.J.Z. acknowledges the U.S. Department of Energy (DE-AR0000177) for financial support of this work. The authors thank Prof. Dr. D. M. Proserpio for discussions related to the topology of **dia** nets. M.H.M. gratefully acknowledges support from the Schlumberger Foundation and its Faculty for the Future Fellowship program. B.S. acknowledges the National Science Foundation (CHE-1152362) and the computational resources made available by an XSEDE Grant (TG-DMR090028).

REFERENCES

(1) Dunne, J. A.; Rao, M.; Sircar, S.; Gorte, R. J.; Myers, A. L. *Langmuir* **1996**, *12*, 5896.
(2) Quinn, D. F.; MacDonald, J. A. *Carbon* **1992**, *30*, 1097.
(3) Wegrzyn, J.; Gurevich, M. *Appl. Energy* **1996**, *55*, 71.
(4) Bhatia, S. K.; Myers, A. L. *Langmuir* **2006**, *22*, 1688.
(5) El-Kaderi, H. M.; Hunt, J. R.; Mendoza-Cortes, J. L.; Cote, A. P.; Taylor, R. E.; O'Keeffe, M.; Yaghi, O. M. *Science* **2007**, *316*, 268.
(6) Moulton, B.; Zaworotko, M. J. *Chem. Rev.* **2001**, *101*, 1629.
(7) MacGillivray, L. R. *Metal-Organic Frameworks: Design and Application*; John Wiley & Sons: Hoboken, NJ, 2010.
(8) Kitagawa, S.; Kitaura, R.; Noro, S.-i. *Angew. Chem., Int. Ed.* **2004**, *43*, 2334.
(9) Koh, K.; Wong-Foy, A. G.; Matzger, A. J. *J. Am. Chem. Soc.* **2009**, *131*, 4184.

(10) Koh, K.; Wong-Foy, A. G.; Matzger, A. J. *Angew. Chem., Int. Ed.* **2008**, *47*, 677.
(11) Farha, O. K.; Eryazici, I.; Jeong, N. C.; Hauser, B. G.; Wilmer, C. E.; Sarjeant, A. A.; Snurr, R. Q.; Nguyen, S. T.; Yazaydin, A. O.; Hupp, J. T. *J. Am. Chem. Soc.* **2012**, *134*, 15016.
(12) Li, J.-R.; Kuppler, R. J.; Zhou, H.-C. *Chem. Soc. Rev.* **2009**, *38*, 1477.
(13) Lee, J.; Farha, O. K.; Roberts, J.; Scheidt, K. A.; Nguyen, S. T.; Hupp, J. T. *Chem. Soc. Rev.* **2009**, *38*, 1450.
(14) Horcajada, P.; Gref, R.; Baati, T.; Allan, P. K.; Maurin, G.; Couvreur, P.; Férey, G.; Morris, R. E.; Serre, C. *Chem. Rev.* **2012**, *112*, 1232.
(15) Givaja, G.; Amo-Ochoa, P.; Gómez-García, C. J.; Zamora, F. *Chem. Soc. Rev.* **2012**, *41*, 115.
(16) Suh, M. P.; Park, H. J.; Prasad, T. K.; Lim, D. W. *Chem. Rev.* **2012**, *112*, 782.
(17) Konstas, K.; Osl, T.; Yang, Y.; Batten, M.; Burke, N.; Hill, A. J.; Hill, M. R. *J. Mater. Chem.* **2012**, *22*, 16698.
(18) Makal, T. A.; Li, J.-R.; Lu, W.; Zhou, H.-C. *Chem. Soc. Rev.* **2012**, *41*, 7761.
(19) Peng, Y.; Krungleviciute, V.; Eryazici, I.; Hupp, J. T.; Farha, O. K.; Yildirim, T. *J. Am. Chem. Soc.* **2013**, *135*, 11887.
(20) Mason, J. A.; Veenstra, M.; Long, J. R. *Chem. Sci.* **2014**, *5*, 32.
(21) Burd, S. D.; Nugent, P. S.; Mohameda, M. H.; Elsaidia, S. K.; Zaworotko, M. J. *CHIMIA: Int. J. Chem.* **2013**, *67*, 372.
(22) Mohamed, M. H.; Elsaidi, S. K.; Wojtas, L.; Pham, T.; Forrest, K. A.; Tudor, B.; Space, B.; Zaworotko, M. J. *J. Am. Chem. Soc.* **2012**, *134*, 19556.
(23) Wilmer, C. E.; Leaf, M.; Lee, C. Y.; Farha, O. K.; Hauser, B. G.; Hupp, J. T.; Snurr, R. Q. *Nat. Chem.* **2012**, *4*, 83.
(24) Zeitler, T. R.; Allendorf, M. D.; Greathouse, J. A. *J. Phys. Chem. C* **2012**, *116*, 3492.
(25) Simon, C. M.; Kim, J.; Lin, L.-C.; Martin, R. L.; Haranczyk, M.; Smit, B. *Phys. Chem. Chem. Phys.* **2014**, *16*, 5499.
(26) Lin, W.; Ma, L.; Evans, O. R. *Chem. Commun.* **2000**, 2263.
(27) Sharma, M. K.; Lama, P.; Bharadwaj, P. K. *Cryst. Growth Des.* **2011**, *11*, 1411.
(28) Carlucci, L.; Ciani, G.; Proserpio, D. M.; Rizzato, S. *Chem.—Eur. J.* **2002**, *8*, 1519.
(29) Caskey, S. R.; Wong-Foy, A. G.; Matzger, A. J. *J. Am. Chem. Soc.* **2008**, *130*, 10870.
(30) Rosi, N. L.; Kim, J.; Eddaoudi, M.; Chen, B.; O'Keeffe, M.; Yaghi, O. M. *J. Am. Chem. Soc.* **2005**, *127*, 1504.
(31) Dietzel, P. D.; Johnsen, R. E.; Blom, R.; Fjellvag, H. *Chem.—Eur. J.* **2008**, *14*, 2389.
(32) Banerjee, R.; Phan, A.; Wang, B.; Knobler, C.; Furukawa, H.; O'Keeffe, M.; Yaghi, O. M. *Science* **2008**, *319*, 939.
(33) Huang, X.-C.; Lin, Y.-Y.; Zhang, J.-P.; Chen, X.-M. *Angew. Chem., Int. Ed.* **2006**, *45*, 1557.
(34) Zaworotko, M. J. *Chem. Soc. Rev.* **1994**, *23*, 283.
(35) Batten, S. R; Robson, R. *Angew. Chem., Int. Ed.* **1998**, *37*, 1460.
(36) Batten, S. R. *CrystEngComm* **2001**, *3*, 67.
(37) Blake, A. J.; Champness, N. R.; Hubberstey, P.; Li, W.-S.; Withersby, M. A.; Schröder, M. *Coord. Chem. Rev.* **1999**, *183*, 117.
(38) Jiang, H.-L.; Makal, T. A.; Zhou, H.-C. *Coord. Chem. Rev.* **2013**, *257*, 2232.
(39) Shekhah, O.; Wang, H.; Paradinas, M.; Ocal, C.; Schupbach, B.; Terfort, A.; Zacher, D.; Fischer, R. A.; Woll, C. *Nat. Mater.* **2009**, *8*, 481.
(40) Zhang, J.; Wojtas, L.; Larsen, R. W.; Eddaoudi, M.; Zaworotko, M. J. *J. Am. Chem. Soc.* **2009**, *131*, 17040.
(41) Bureekaew, S.; Sato, H.; Matsuda, R.; Kubota, Y.; Hirose, R.; Kim, J.; Kato, K.; Takata, M.; Kitagawa, S. *Angew. Chem., Int. Ed.* **2010**, *49*, 7660.
(42) Desiraju, G. R. *Angew. Chem., Int. Ed.* **2007**, *46*, 8342.
(43) Blatov, V. A.; Shevchenko, A. P.; Serezhkin, V. N. *J. Struct. Chem.* **1994**, *34*, 820.
(44) Blatov, V. A. *IUCr CompComm Newsl.* **2006**, *7*, 4–38, http://www.topos.samsu.ru.
(45) Eddaoudi, M.; Kim, J.; Rosi, N.; Vodak, D.; Wachter, J.; O'Keeffe, M.; Yaghi, O. M. *Science* **2002**, *295*, 469.
(46) Zhang, Y.-B.; Zhou, H.-L.; Lin, R.-B.; Zhang, C.; Lin, J.-B.; Zhang, J.-P.; Chen, X.-M. *Nat. Commun.* **2012**, *3*, 642.
(47) Wu, H.; Zhou, W.; Yildirim, T. *J. Am. Chem. Soc.* **2009**, *131*, 4995.
(48) Furukawa, H.; Yaghi, O. M. *J. Am. Chem. Soc.* **2009**, *131*, 8875.
(49) Martin, R. L.; Shahrak, M. N.; Swisher, J. A.; Simon, C. M.; Sculley, J. P.; Zhou, H.-C.; Smit, B.; Haranczyk, M. *J. Phys. Chem. C* **2013**, *117*, 20037.